Mathematical Modeling of the Pituitary–Thyroid Feedback Loop: Role of a TSH-T$_3$-Shunt and Sensitivity Analysis

Julian Berberich[1], Johannes W. Dietrich[2,3,4], Rudolf Hoermann[5] and Matthias A. Müller[1]*

[1]Institute for Systems Theory and Automatic Control, University of Stuttgart, Stuttgart, Germany, [2]Medical Department I, Endocrinology and Diabetology, Bergmannsheil University Hospitals, Ruhr University of Bochum, Bochum, Germany, [3]Ruhr Center for Rare Diseases (CeSER), Ruhr University of Bochum, Bochum, Germany, [4]Ruhr Center for Rare Diseases (CeSER), Witten/Herdecke University, Bochum, Germany, [5]Private Consultancy Research & Development, Yandina, QLD, Australia

Despite significant progress in assay technology, diagnosis of functional thyroid disorders may still be a challenge, as illustrated by the vague upper limit of the reference range for serum thyrotropin (*TSH*). Diagnostical problems also apply to subjects affected by syndrome T, i.e., those 10% of hypothyroid patients who continue to suffer from poor quality of life despite normal *TSH* concentrations under substitution therapy with levothyroxine (*L-T$_4$*). In this paper, we extend a mathematical model of the pituitary–thyroid feedback loop in order to improve the understanding of thyroid hormone homeostasis. In particular, we incorporate a *TSH-T$_3$*-shunt inside the thyroid, whose existence has recently been demonstrated in several clinical studies. The resulting extended model shows good accordance with various clinical observations, such as a circadian rhythm in free peripheral triiodothyronine (*FT$_3$*). Furthermore, we perform a sensitivity analysis of the derived model, revealing the dependence of *TSH* and hormone concentrations on different system parameters. The results have implications for clinical interpretation of thyroid tests, e.g., in the differential diagnosis of subclinical hypothyroidism.

Keywords: thyroid hormones, pituitary–thyroid feedback loop, mathematical modeling, diagnosis, TSH-T$_3$-shunt, sensitivity analysis

1. INTRODUCTION

In recent years, the mathematical modeling of human thyroid hormone homeostasis via the hypothalamic–pituitary–thyroid feedback loop has received an increasing amount of attention. Starting from early phenomenological models, more precise models have been developed based on molecular and pharmacokinetic data, see, e.g., Ref. (1–3, 4–6) for recent surveys on existing modeling approaches. These mathematical models can give important insight into the functionality of the hypothalamic–pituitary–thyroid axis and can be used to simulate the dynamic behavior of thyroidal hormone concentrations under different (euthyroid and non-euthyroid) conditions, and sometimes also for clinical decision-making (7). Furthermore, in Ref. (8), a method is proposed to compute personalized euthyroid setpoints that can be used for individualized diagnosis and treatment of thyroid diseases. While this static model is appealing due to its simplicity (only two

parameter values have to be estimated), it does not consider any dynamic phenomena in the HPT axis, which are, however, of great importance for a deepened understanding of the HPT axis and ultimately the development of personalized optimal medication strategies. Another drawback is the absence of any consideration of T_3, which has been shown to be significant not only as a key actor in the hypothalamic–pituitary–thyroid feedback loop (4, 9) but also in maintaining a good quality of life (5).

The main objective of this paper is an improved mathematical modeling of the HPT axis in order to obtain a more detailed understanding of the dynamic phenomena occurring in thyroid hormone homeostasis. In particular, as a first contribution, we extend the model originally developed in Ref. (1, 2) in order to incorporate new insights obtained through several recent clinical studies. In particular, we incorporate a direct TSH-T_3 path inside the thyroid, accounting for the central T_3 production by the thyroid. Existence of such a TSH-T_3-shunt was hypothesized and demonstrated in several experiments and clinical observations (10–15). In Ref. (10), it was shown that L-T_4-treated athyreotic patients exhibit decreased FT_3 concentrations despite normal free thyroxine (FT_4) levels, which would not be the case if peripheral FT_3 was mainly produced by deiodination of peripheral FT_4. Furthermore, the sum activity of step-up deiodinases (G_D) is positively correlated with the TSH concentration (11) and with the thyroidal volume (12) and significantly decreases after thyroidectomy. These observations suggest that besides the peripheral T_4/T_3 conversion, also TSH-stimulated deiodinases inside the thyroid contribute to the total T_3 production. In our work, we show that the extended model including such a TSH-T_3-shunt is in good accordance with various clinical observations. For example, we show that the FT_3 concentration shows a clear circadian pattern, as was observed *in vivo* in Ref. (16). Notably, this is not the case in the previous model, which did not include the TSH-T_3-shunt.

As a second main contribution of this paper, we perform a sensitivity analysis of the derived model. Loosely speaking, the (first-order) sensitivities are a measure for how "sensitive" certain system states (i.e., TSH or hormone concentrations) are with respect to changes in certain parameters (such as, e.g., the thyroid's secretory capacity G_T). These sensitivities reveal structural insight into the functionality of the hypothalamic–pituitary–thyroid axis and can provide explanations for certain clinical observations. For example, we show that the sensitivity of TSH with respect to G_T is much higher for low values of G_T (i.e., in hypothyroidism) than for high values of G_T (i.e., in hyperthyroidism). This fact can be used to explain why in clinical practice, TSH concentrations may significantly vary beyond the upper limit of the reference range despite normal thyroid function.

The remainder of this paper is structured as follows. Section 2 presents the extended mathematical model and discusses the identification of the required (additional) parameters. In Section 3, we show simulation results of the derived model and discuss the observed properties (such as the existence of a circadian rhythm in FT_3 concentrations). A sensitivity analysis of TSH, FT_4, and FT_3 concentrations with respect to different parameters is performed in Section 4. Finally, we conclude the paper in Section 5.

2. PRESENTATION OF THE EXTENDED MODEL AND PARAMETER IDENTIFICATION

As outlined above, several clinical observations have led to the hypothesis that a direct, TSH-stimulated path exists for T_3 production inside the thyroid, which we now incorporate into the mathematical model from Ref. (1, 2). The extended model including this TSH-T_3-shunt is illustrated in **Figure 1**, see Section S1 in the Supplementary Material for a mathematical description of the underlying differential equations. To this end, both intrathyroidal conversion of T_4 into T_3 via type 1 and 2 $5'$-deiodinases as well as a direct synthesis of T_3 are modeled (see upper three blocks in the "Thyroid" block in **Figure 1**). Both mechanisms are stimulated by TSH and modeled via nonlinear Michaelis–Menten–Hill kinetics, see Section S1 in the Supplementary Material for further details.

Most of the parameters of the extended model can be taken from the model in Ref. (1, 2), where the parameters have been estimated according to known physical quantities (such as the half-life period of certain substances, etc.) or have been identified using data measured *in vivo*. A detailed listing of these parameters can be found in the Tables S1–S3 in Supplementary Material. Some of the parameters were calibrated according to average population data, and hence the resulting model can be interpreted to be a functional model of some generic euthyroid subject. Clearly, personalized model identification would be highly valuable for individualized clinical decision-making and the development of personalized optimal medication strategies. For this, however, sufficient data such as individual dynamic trajectories of hormone concentrations would be needed to avoid overfitting. We note that, while the present report deals mainly with average population data, the observed phenomena are in good accordance with individual samples (9).

For the extended model, the new parameters G_{T3} and k have to be determined. Also, the sum activity of the type 1 $5'$-deiodinase, G_{D1}, has to be re-estimated. This is the case since the extended model considers the additional T_3 secretion inside the thyroid, while in the original model, G_{D1} was calibrated by only considering peripheral T_3 production, and hence G_{D1} had been estimated too high. In order to obtain the parameters G_{T3} and G_{D1}, a least squares estimation was performed, fitting the FT_3-output of the presented model to FT_3 measurements of a clinical study. Although there is no unique solution in case that only single FT_3 measurements are available, it provides a set of optimal parameters, which could be further reduced to a unique solution if additional measurements were available (compare the detailed discussion below). In order to perform the least squares estimation, the equilibrium FT_3 level predicted by the extended model, in the following denoted by $FT_{3,eq}$, can be computed in dependence of the parameters by solving a cubic polynomial (see Section S1 in the Supplementary Material for a more detailed description). For this computation, we set TRH to a constant value (later, for the dynamic analysis TRH is varying in a sinusoidal fashion). This equilibrium value is then fitted in a least-squares sense to real measurement data resulting from 1,121 untreated patients of the clinical study in Ref. (11). In particular, this is
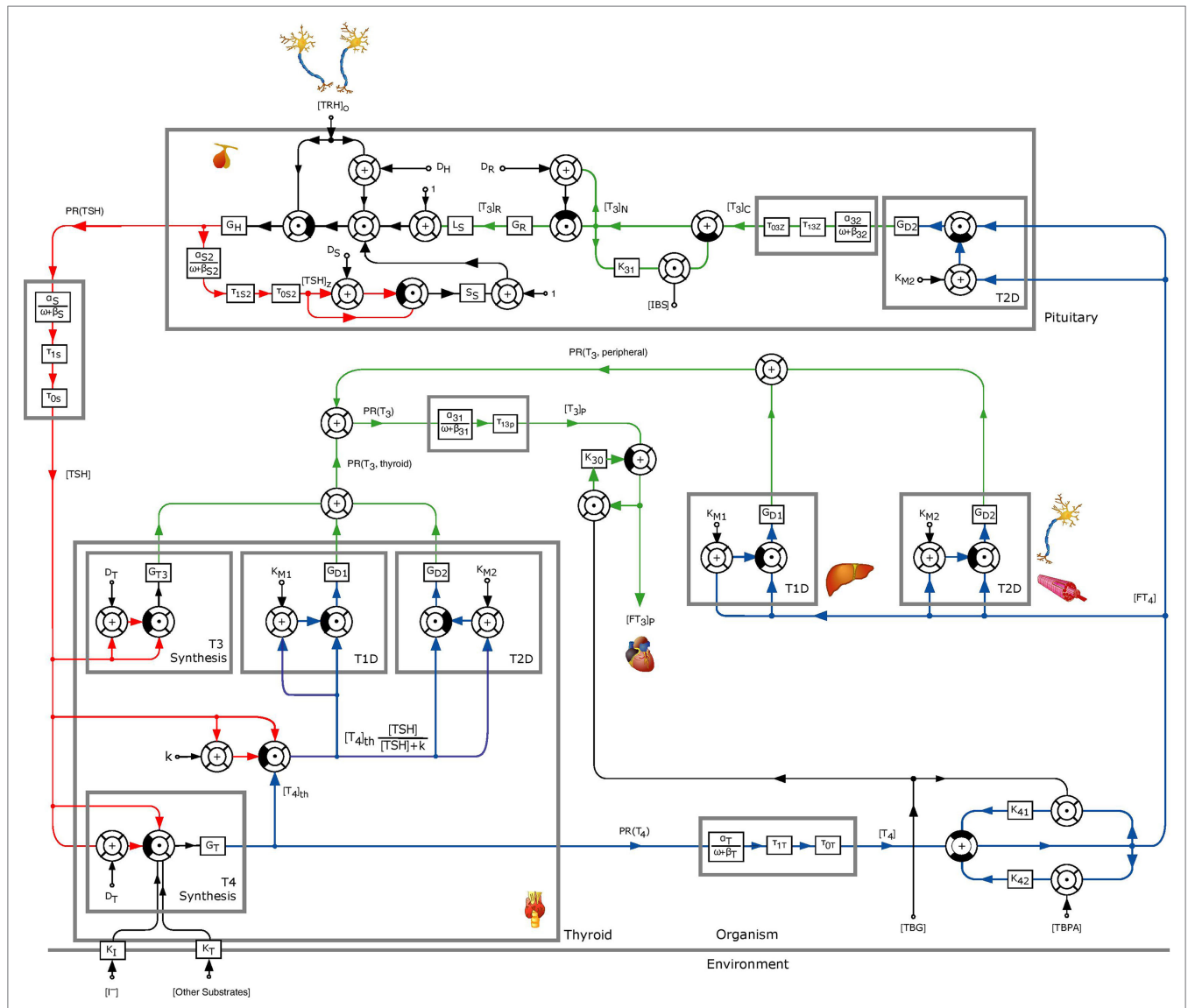
FIGURE 1 | Block diagram of the thyrotropic feedback control loop with an additional *TSH-T3-shunt*, adapted from Ref. (1, 2). Except for G_{T3}, k, and G_{D1}, all parameters were adopted from the model in Ref. (1, 2). The parameters G_{D1} and G_{T3} were estimated to obtain an optimal (in a least squares sense) fit to measured *in vivo* FT_3-concentrations. To this end, the value of k was normalized to 1 mU/l.
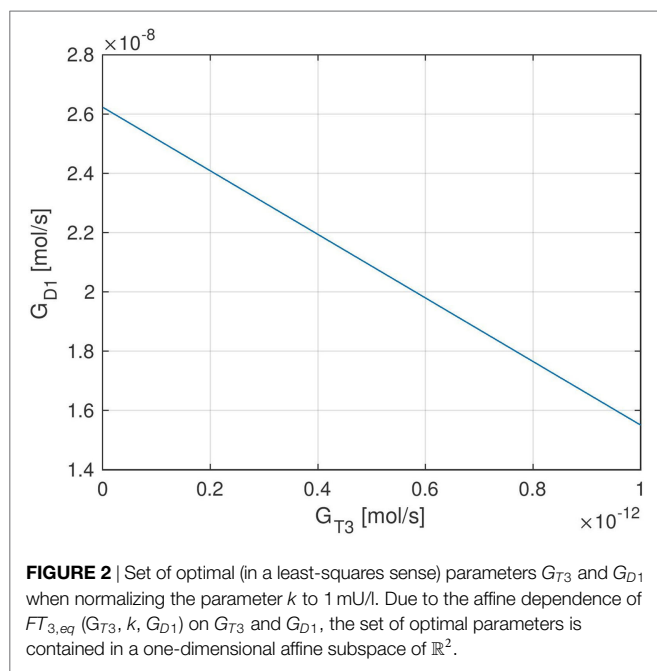
achieved by minimizing the following cost function with respect to the parameters G_{T3}, k, and G_{D1}:

$$J\left(G_{T3}, k, G_{D1}\right) = \sum_{i=1}^{1121} \left(FT_{3,i} - FT_{3,eq}\left(G_{T3}, k, G_{D1}\right)\right)^2 \quad (1)$$

Here, $FT_{3,i}$ denotes the measured FT_3-concentration of the i-th patient, and $FT_{3,eq}\left(G_{T3}, k, G_{D1}\right)$ is the equilibrium FT_3-level predicted by the model depending on the parameters G_{T3}, k, and G_{D1}. The other parameters that are needed to compute $FT_{3,eq}$ are adopted from Ref. (1) (see Tables S1–S3 in the Supplementary Material). The optimal solution to the above optimization problem can be determined analytically and is given by $FT_{3,eq}\left(G_{T3}, k, G_{D1}\right) = \overline{FT_3}$, where $\overline{FT_3}$ is the mean value of the 1,121 FT_3 measurements. Using the derived formula for

$FT_{3,eq}\left(G_{T3}, k, G_{D1}\right)$ (see Section S1 in the Supplementary Material), this results in different (infinitely many) optimal parameter combinations for G_{T3}, k, and G_{D1}. For example, normalizing k to $1\frac{mU}{l}$ (which will be used in the following), the optimal parameter combinations for G_{T3} and G_{D1} can be seen in **Figure 2**.

Different (optimal) parameter combinations for G_{T3} and G_{D1} result in different fractions of thyroidal and peripheral T_3 production. For example, $G_{D1} = 22\frac{nmol}{s}$ and $G_{T3} = 394\frac{fmol}{s}$ approximately lead to 80% T_3 production from peripheral conversion of FT_4 and approximately 20% T_3 production from intrathyroidal secretion, corresponding to the values suggested by Ref. (17, 18). On the other hand, also, a higher or lower fraction of intrathyroidal T_3 production is possible, depending on the values of G_{T3} and G_{D1}. In particular, higher values of G_{T3} and lower values for G_{D1} result in a higher fraction of intrathyroidal T_3 production

FIGURE 2 | Set of optimal (in a least-squares sense) parameters G_{T3} and G_{D1} when normalizing the parameter k to 1 mU/l. Due to the affine dependence of $FT_{3,eq}$ (G_{T3}, k, G_{D1}) on G_{T3} and G_{D1}, the set of optimal parameters is contained in a one-dimensional affine subspace of $\mathbb{R}^2$.

and vice versa. For the dynamic simulation of the model and the sensitivity analysis in the following sections, we (mostly) use the values $G_{D1} = 22\frac{nmol}{s}$ and $G_{T3} = 394\frac{fmol}{s}$, and we comment when certain results qualitatively change if other parameter values for G_{D1} and G_{T3} are used.

The above discussed non-uniqueness in the optimal parameter fit is due to the fact that the model is not fully identifiable given the measured data. Namely, FT_3 is the only hormone that is affected by the parameters G_{T3}, k, and G_{D1}, and we only have stationary measurements available. Furthermore, in the above estimation, we made the simplifying assumption that peripheral and thyroidal deiodinase activities (G_{D1} and G_{D2}) are the same, which might in general not be the case. Identifying the corresponding parameters separately would result in a possibly better parameterized model, which is, however, again not possible given only the stationary FT_3 measurements. On the other hand, if we had additional data such as dynamic hormone concentration trajectories or additional measurements (e.g., intrathyroidal hormone concentrations), the above described non-uniqueness in the parameter estimation could be removed and also different parameter values for thyroidal and peripheral deiodinase activity could be identified, allowing for a more exact parameterization of the model. This would be an interesting topic for future research, however, such *in vivo* data are difficult to obtain and are typically not available. Moreover, the presented model does not consider membrane transport processes between thyroidal and peripheral tissue. Incorporating such processes by means of a compartment model would further increase the quality of our model, yet, this would yield additional parameters, which had to be identified. Nevertheless, as we will show in the following sections, the extended model with the parameters as identified in this section is a clear improvement compared to the previous model, allowing for a better reproduction and interpretation of various clinically observed phenomena.

3. DYNAMIC PROPERTIES OF THE EXTENDED MODEL

In the following, we simulate the extended model and analyze and interpret the obtained results. First, some simulation runs are carried out to illustrate the role of the TSH-T_3-shunt in obtaining a circadian rhythm in the FT_3-concentration. Afterwards, we investigate the delay between TSH and FT_3, which has been observed in several clinical studies [e.g., Ref. (16, 19)].
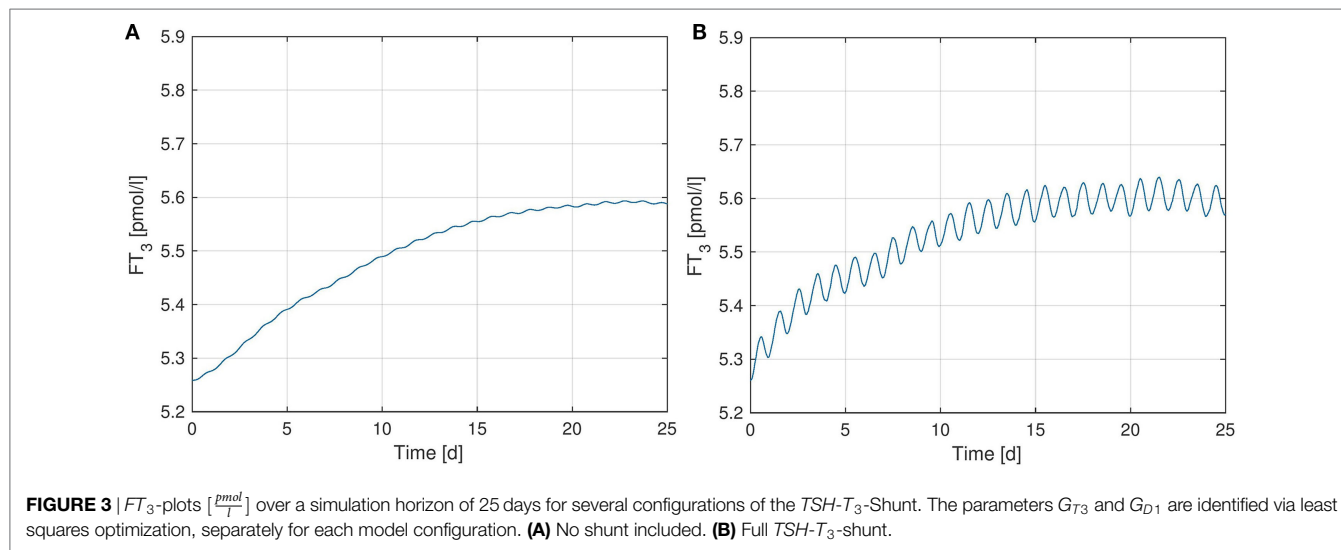
3.1. Dynamic Simulation

As detailed in the previous section, the intrathyroidal T_3 secretion is composed of two mechanisms, namely intrathyroidal conversion of T_4 into T_3 via type 1 and 2 5′-deiodinases (upper middle and right block inside the thyroid in **Figure 1**) as well as a direct synthesis of T_3 (upper left block inside the thyroid in **Figure 1**). In the dynamic simulation using the parameters as identified in Section 2, the intrathyroidal contribution to the total T_3 secretion rate was composed as follows:

$$\frac{Output\ of\ block\ ''T3\ Synthesis''}{PR(T_3,\ thyroid)} = 79.7\%$$

$$\frac{Output\ of\ block\ ''T1D''}{PR(T_3,\ thyroid)} = 20.3\%$$

$$\frac{Output\ of\ block\ ''T2D''}{PR(T_3,\ thyroid)} = 0.002\%$$

Hence, with the parameters identified in Section 2, the main thyroidal source to T_3-production is direct T_3-synthesis via Michaelis–Menten–Hill kinetics, represented by the block "T3 Synthesis" in **Figure 1**. On the other hand, deiodination by type 2 5′-deiodinases has a negligible effect only, since the sum activity of type 2 5′-deiodinases is much smaller compared to that of type 1 5′-deiodinases. In case that a different optimal combination of parameters G_{T3} and G_{D1} is used (compare Section 2), the above results change accordingly, i.e., a higher value of G_{D1} yields a higher contribution of the deiodination by type 1 5′-deiodinases to the thyroidal T_3-production. However, this also causes a change in the ratio between thyroidal and peripheral T_3 production, as discussed in Section 2.

Figure 3 shows simulated FT_3-plots, where we further investigated the effect of the TSH-T_3-shunt on the dynamic behavior of FT_3.[1] In particular, **Figure 3A** shows simulation results using the previous model from Ref. (1) without the TSH-T_3-shunt whereas in **Figure 3B**, the full TSH-T_3-shunt as described in the previous section is included. For each of the two scenarios (i.e., for the corresponding models), we separately identified the (in a least-squares-sense) optimal parameter(s): G_{D1} for the model corresponding to **Figure 3A** and G_{D1} as well as G_{T3} for the model corresponding to **Figure 3B**. The exact values of these parameters for the different model configurations can be seen in Table S4 in Supplementary Material.

---

[1]The initial hormone values for the simulations shown in **Figure 3** (and for all subsequent simulation runs) were chosen as the stationary mean values of the model, i.e. as the hormone values the model yields for a constant TRH input. Note, however, that the choice of initial values is not particularly important for the simulation, as long as they lie somewhere in the euthyroid range.

FIGURE 3 | FT_3-plots $\left[\frac{pmol}{l}\right]$ over a simulation horizon of 25 days for several configurations of the TSH-T_3-Shunt. The parameters G_{T3} and G_{D1} are identified via least squares optimization, separately for each model configuration. **(A)** No shunt included. **(B)** Full TSH-T_3-shunt.

We observe that the TSH-T_3-shunt causes a clear circadian oscillation in the FT_3 concentration, which is not (or only very weakly) present without considering intrathyroidal T_3 secretion. Such a circadian rhythm in FT_3 concentration has been observed *in vivo* in several clinical studies [see, e.g., Ref. (16, 19)], and hence our simulation results again support existence of the TSH-T_3-shunt.

Quantitatively, the oscillation amplitude of the measured *in vivo* FT_3 concentration in Ref. (16) is approximately six times as big as the amplitude observed in the simulated model (see **Figure 3B**). This difference might be due to the assumptions we made for the identification in Section 2 (same values for G_{D1}, G_{D2}, K_{M1}, and K_{M2} inside the thyroid and the peripheral tissue). Namely, if thyroidal deiodination activity and/or G_{T3} were higher than computed in Section 2, without increasing the peripheral deiodination activity as well, we would obtain a larger oscillation amplitude in FT_3 concentration. Nevertheless, the fact that a clear circadian pattern arises in the simulations when including the TSH-T_3-shunt into the model is a clear indicator supporting both its existence as well as the fact that thyroidal T_3 secretion is stimulated by TSH.

3.2. Delay of FT_3 w.r.t. TSH

The authors in Ref. (16) make the observation that *in vivo* FT_3-measurements follow a clear circadian pattern, which is approximately 90 min delayed w.r.t. TSH; this number can also vary between different individuals (19). As already mentioned in the previous section, the FT_3-level obtained by the model in **Figure 1** including intrathyroidal T_3-secretion shows a clear circadian pattern. In this section, we investigate how the delay between TSH and FT_3 in the presented model is influenced by this newly incorporated mechanism.

A dynamic simulation with the same setup as in Section 3.1 yields the following: when incorporating the TSH-T_3-shunt into the model, FT_3 is delayed w.r.t. TSH by approximately 6 h, whereas the delay amounts to 13 h in the previous model, which did not incorporate this mechanism. These observed values can be explained as follows. The phase shift between FT_3 and TSH in

our model mainly results from the first order lag elements $\frac{\alpha}{i\omega + \beta}$ modeling peripheral T_3 and T_4 secretion (i.e., the ones with parameters α_{31}, β_{31}, and α_T, β_T, respectively in **Figure 1**). The phase shift of the output signal of such a first order lag element for a given sinusoidal input signal with frequency ω depends on the parameter β and is given as follows:

$$phase = arctan\left(-\frac{\omega}{\beta}\right). \tag{2}$$

In our case, $\omega = \frac{2\pi}{T}$ where $T = 86,400\,s$ is the circadian period of 1 day. The delay between the output and input signal is now computed by simply relating the phase shift to the period length T: $delay = -phase \cdot \frac{T}{2\pi}$. For the given parameter values α_{31}, β_{31}, and α_T, β_T of T_3- and T_4-generation, respectively, we obtain a delay of approximately 5.5 and 6 h, respectively.

The above observed delay of FT_3 w.r.t. TSH can now be explained as follows. In the previous model not including the TSH-T_3-shunt, the circadian oscillation has to pass through both first order lag elements for peripheral T_4 and T_3 production, resulting in a high delay w.r.t. TSH. On the other hand, the fraction of T_3 secreted inside the thyroid does not exhibit the delay caused by peripheral T_4 production and hence exhibits a much shorter delay w.r.t. TSH. Interestingly, the observed delay of total T_3 (approximately 6 h) mainly seems to be determined by the shorter one resulting from intrathyroidal T_3 production, although approximately 80% of the total T_3-production results from peripheral FT_4-deiodination and only 20% from intrathyroidal secretion. The reason for this is that as explained above, the circadian rhythm of FT_3 is mainly induced by intrathyroidal T_3 secretion. Namely, the ratio of the amplitude and the mean value equals 0.3% for the peripheral T_3 production rate $PR(T_3, peripheral)$ and 23% for the thyroidal T_3 production rate $PR(T_3, thyroid)$. Thus, the phase of FT_3 is almost solely characterized by the phase of thyroidal T_3-production, and hence the delay of FT_3 w.r.t. TSH is determined by the phase shift of only one first order lag element when the shunt is included, compared to two without the shunt. To conclude, the inclusion of the TSH-T_3-shunt into the model significantly reduces the delay of FT_3 w.r.t. TSH. While
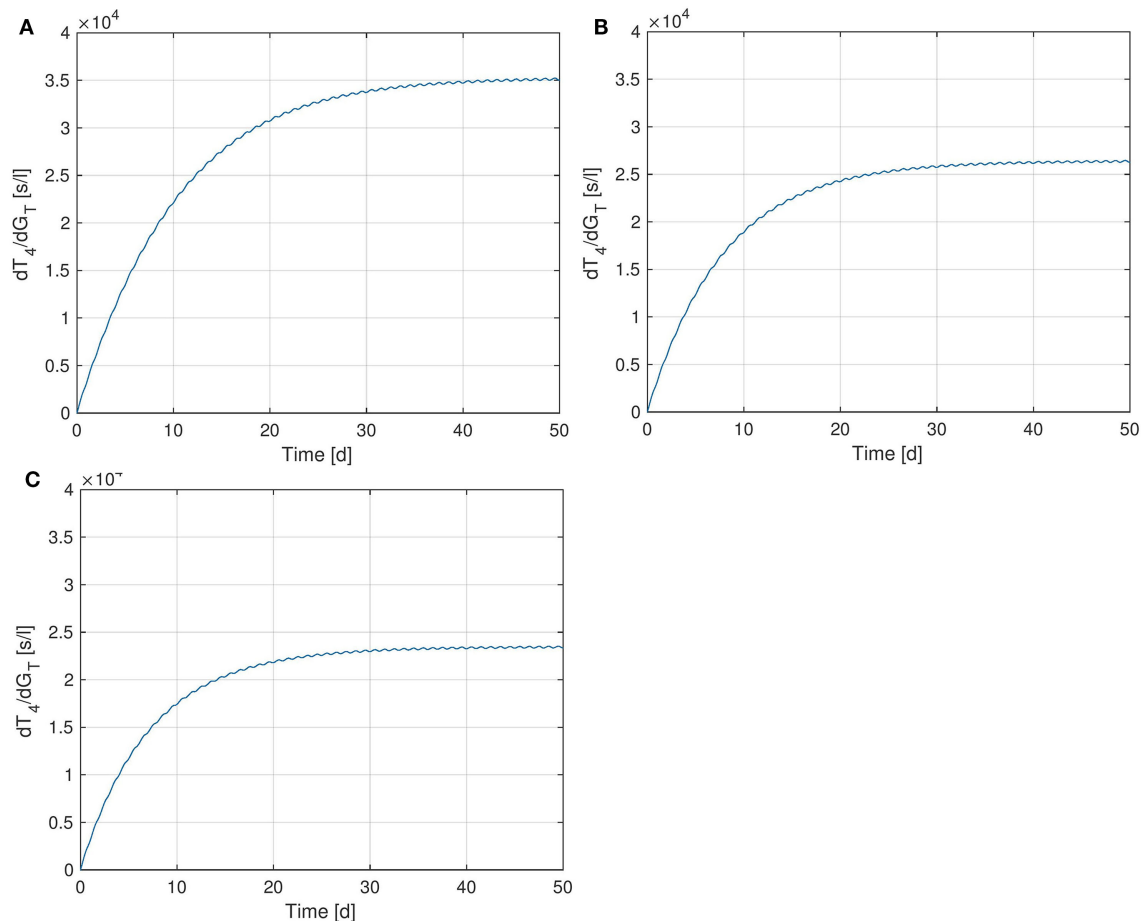
FIGURE 4 | Sensitivity of T_4 w.r.t. G_T for different values of G_T. **(A)** $G_T = 1.2 \cdot 10^{-12} \frac{mol}{s}$, **(B)** $G_T = 3.375 \cdot 10^{-12} \frac{mol}{s}$ - nominal value, **(C)** $G_T = 5 \cdot 10^{-12} \frac{mol}{s}$.

the absolute numbers are still too high compared to the observed *in vivo* delays (16, 19), this is again a clear indicator for the existence of the *TSH-T$_3$-shunt*.

4. SENSITIVITY ANALYSIS AND STATIONARY DEPENDENCIES

In this section, we perform a sensitivity analysis of the previously presented mathematical model of the hypothala-mic–pituitary–thyroid feedback loop (see **Figure 1**). Sensitivity analysis is a tool for determining how a certain parameter influences the trajectories resulting from simulation of the model, i.e., from the solution of the underlying system of differential equations, and in particular, how "sensitive" these trajectories are with respect to certain parameter changes. In the following, we give a brief non-formal introduction to sensitivity analysis and refer to the Section S2 in Supplementary Material for a more complete and formal description.

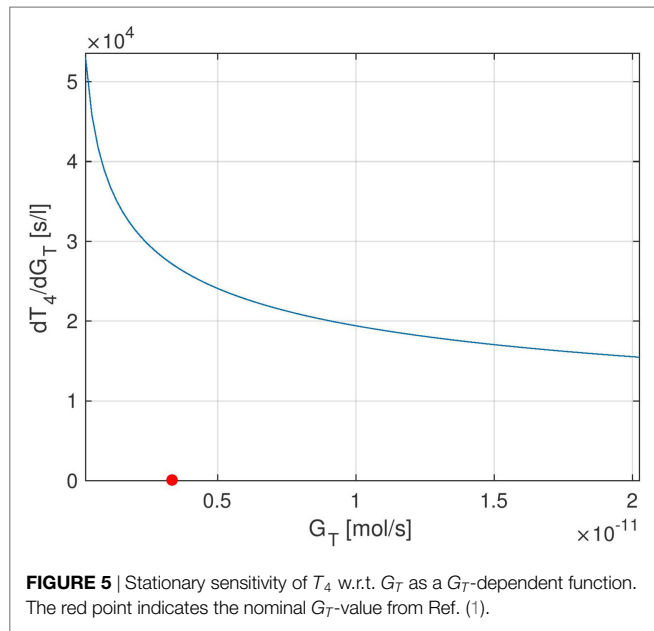To define sensitivities, consider the following vector-valued ordinary differential equation with parameter vector p:

$$\dot{x} = f(t, x, p), \quad x(t_0) = x_0. \tag{3}$$

The first-order sensitivity function[2] is now defined as $S(t) = \left.\frac{\partial x(t,p)}{\partial p}\right|_{p=p_0}$, where p_0 is some nominal (constant) parameter value. The sensitivity function $S(t)$ is a time-dependent matrix with as many rows as the dimension of x and as many columns as the dimension of p. Under some assumptions (smoothness, existence of solutions, ...), it can be shown that S satisfies the following differential equation, which is solved simultaneously with the state equation (3), see Ref. (20).

$$\dot{x} = f(t, x, p_0)$$
$$\dot{S} = \left[\frac{\partial f(t, x, p)}{\partial x}\right]_{p=p_0} \cdot S + \left[\frac{\partial f(t, x, p)}{\partial p}\right]_{p=p_0}$$
$$x(t_0) = x_0, \quad S(t_0) = 0. \tag{4}$$

The initial sensitivity, i.e., $S(t_0)$, is set to zero since the states' initial values are independent of the parameters. The above presented mathematical model of the hypothalamic–pituitary–thyroid feedback loop (see **Figure 1**) includes 36 parameters. With 5 states

---

[2]The definition of S is such that it measures the sensitivity locally around a given nominal parameter value p_0 along a solution trajectory of system (3), which is why it is typically called *first-order* sensitivity. In the following, for brevity, we just use the term sensitivity.

FIGURE 5 | Stationary sensitivity of T_4 w.r.t. G_T as a G_T-dependent function. The red point indicates the nominal G_T-value from Ref. (1).

(pituitary TSH and T_3 as well as peripheral TSH, T_4, and T_3 concentrations), this makes a total of 180 different sensitivity curves - for one specific nominal parameter configuration p_0. In the following, we only analyze a few interesting curves to obtain some new insights. Of course, if desired, one could analogously analyze further sensitivities of other state and parameter pairs. In order to be able to employ the standard sensitivity analysis tools described above, the time delays in the hypothalamic–pituitary–thyroid (HPT) axis model are neglected.

4.1. Sensitivity of T_4 w.r.t. G_T

We start by examining the sensitivity of peripheral T_4 with respect to the thyroid's secretory capacity G_T. In **Figure 4**, several plots of the sensitivity $\frac{\partial T_4}{\partial G_T}(t)$ are shown with different G_T-values, corresponding to different parameter values p_0 in equation (4).[3] Note that the sensitivity curves do not exhibit large variations over the day, i.e., only show a small circadian oscillation. It can be seen that different values of G_T result in different sensitivities of T_4 with respect to G_T. For example, a low value of G_T (which can be seen as a simple modeling of hypothyroidism) causes an increase of the sensitivity, whereas a high G_T value (which can be seen as a simple modeling of hyperthyroidism) causes a decrease of the sensitivity. This means that larger fluctuations in T_4 can be expected at the lower end of its euthyroid reference range (compare Section 4.3). This observation can compactly be expressed for a wide range of G_T-values by investigating the stationary sensitivity (i.e., $\lim_{t \to \infty} \frac{\partial T_4}{\partial G_T}(t)$). **Figure 5** shows it as a function of the parameter G_T. A comparison between **Figures 4** and **5** shows that the stationary sensitivity, indeed, is the limit of the sensitivity curve for $t \to \infty$.

---

[3]For the simulation runs shown in **Figure 4** and in all subsequent dynamic sensitivity curves, the initial sensitivity is set to zero [cf. also the initial condition $S(t_0)=0$ in (4)]

4.2. Sensitivity of TSH w.r.t. TRH

It is interesting to observe that the Ultra-Short-Feedback loop (i.e., the lower left part inside the pituitary in **Figure 1**, compare Ref. (2)) has a significant influence on the sensitivity of TSH w.r.t. TRH. **Figure 6** shows the curves of this sensitivity for different values of S_s. It can be seen that an increase in S_s causes a decrease in the sensitivity.

In the considered HPT axis model, TRH is treated as a time-dependent input that comes from the hypothalamus. A disturbance in the system could lead to a change in the TRH concentration arriving at the pituitary. Apparently, the Ultra-Short-Feedback increases the robustness of the TSH production w.r.t. changes in portal TRH. If the additional feedback is absent (i.e., $S_s = 0$), the sensitivity is significantly higher than in the nominal case ($S_S = 100 \frac{l}{mU}$).
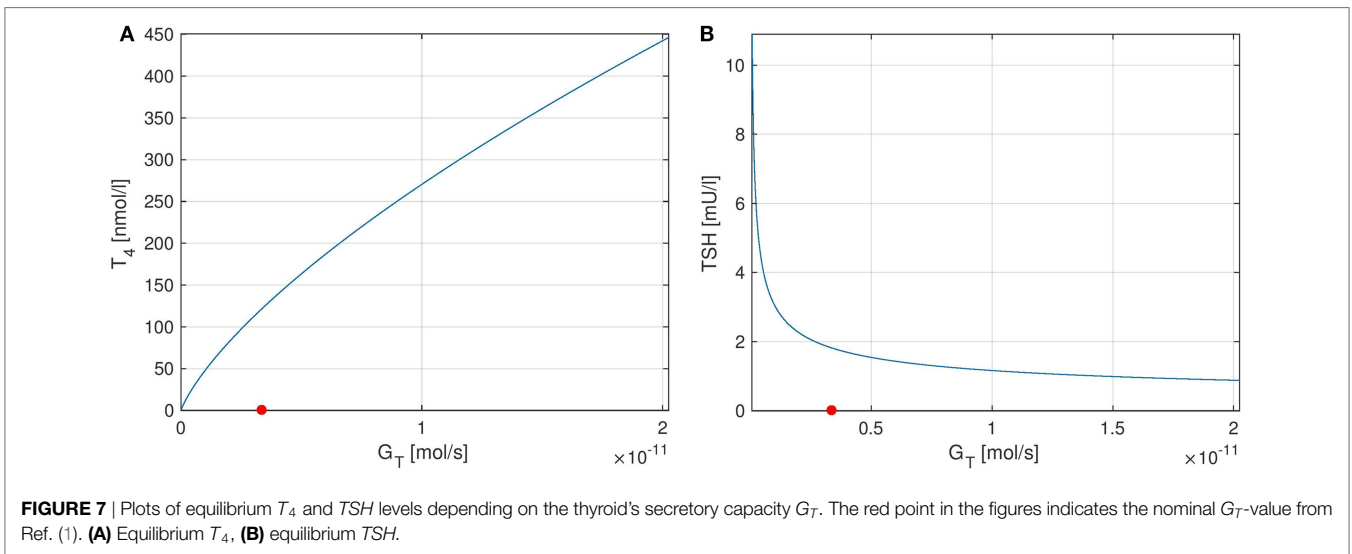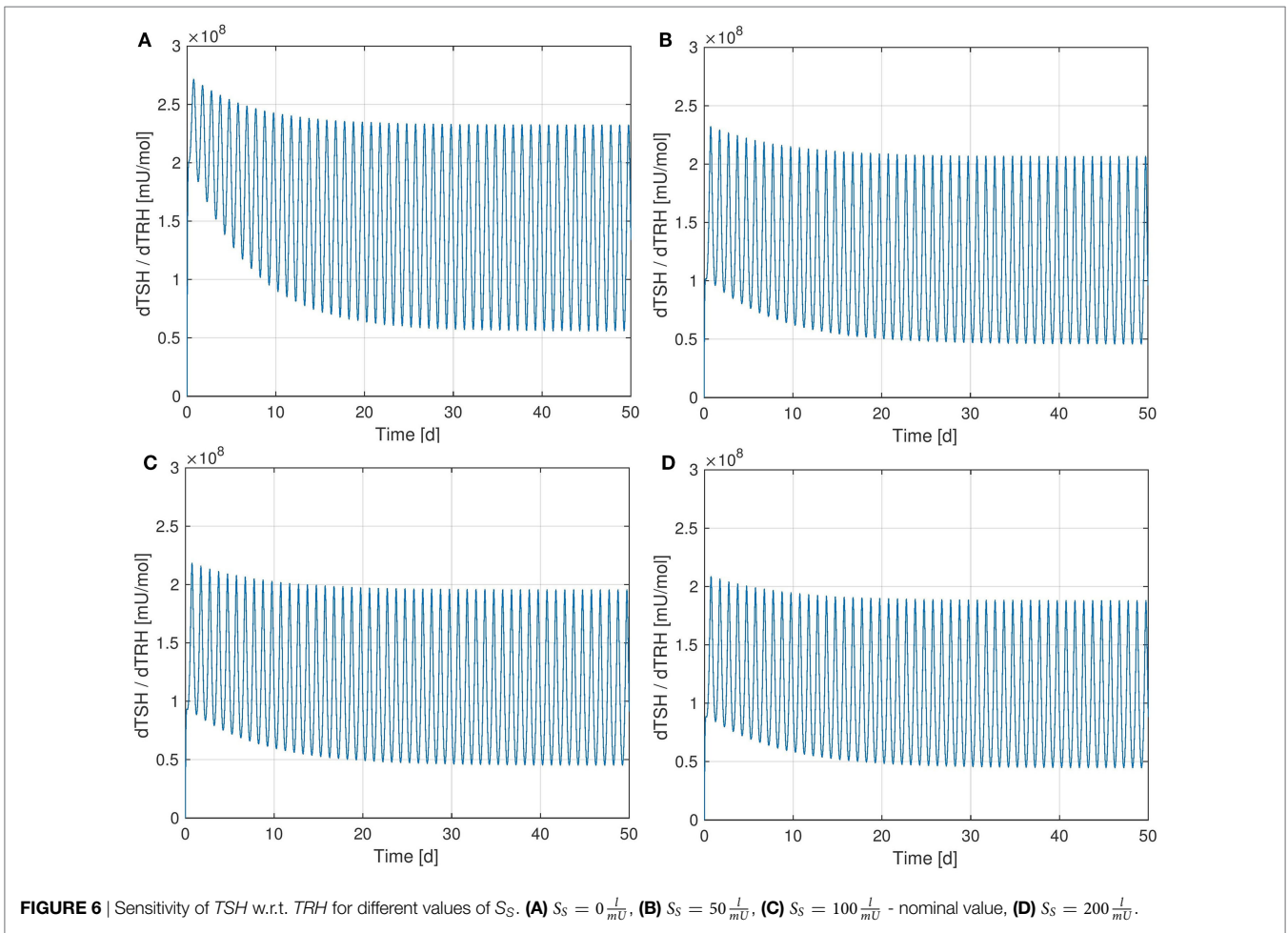
4.3. Stationary Dependencies of TSH and T_4 on G_T

In the following, the influence of the thyroid's secretory capacity G_T on the equilibrium concentrations of TSH and T_4 is analyzed. To this end, we solve the system's stationary equations (i.e., for $t \to \infty$) for the different hormones and plot the resulting equilibrium hormone levels as functions of G_T. The slopes of these functions are exactly the entries of the stationary sensitivity matrix $\lim_{t \to \infty} S(t)$. For example, the stationary sensitivity $\lim_{t \to \infty} \frac{\partial T_4}{\partial G_T}(t)$ for a given value of G_T is equal to the derivative of the curve $T_4(G_T)$ w.r.t. G_T, which we treat in the following.

The curves of T_4 and TSH depending on G_T are shown in **Figure 7**. One can see that the parameter G_T can be used as a measure of hypo- or hyperthyroidism (1). The equilibrium T_4-concentration increases almost linearly with G_T. Furthermore, we have high TSH-levels for low values of G_T, i.e., in hypothyroidism, and vice versa. This is a well-known fact, which is usually used in clinical decision-making for the determination of subclinical thyroid diseases. Another interesting fact is that the magnitude of the sensitivity of TSH w.r.t. G_T (which is the slope of **Figure 7B**) is high for low values of G_T and vice versa. This means that TSH is much more sensitive to fluctuations in the thyroid's secretory capacity if G_T is low. This fact can be used to interpret the following clinical observation. In practice, TSH concentrations may be misleading, especially, if located slightly above the vague upper limit of the reference range. A reason for this could be that as discussed above, TSH is much more sensitive to fluctuations in the thyroid's secretory capacity (e.g., due to different iodine supply and other influences) at the upper limit of its (euthyroid) reference range than at its lower limit.

4.4. Sensitivity of FT_3 w.r.t. G_T

Finally, we perform a sensitivity analysis for FT_3 w.r.t. the parameter G_T. **Figure 8** shows the sensitivity curve, where in **Figure 8A**, the extended model including the TSH-T_3-shunt was used, whereas **Figure 8B** uses the previous model without the shunt. It can be seen that the sensitivity of FT_3 w.r.t. G_T decreases when the shunt is included. This is to be expected since in the extended model, a direct synthesis of T_3 (upper left block inside the thyroid in **Figure 1**) is included, which is independent of

FIGURE 6 | Sensitivity of *TSH* w.r.t. *TRH* for different values of S_S. **(A)** $S_S = 0 \frac{l}{mU}$, **(B)** $S_S = 50 \frac{l}{mU}$, **(C)** $S_S = 100 \frac{l}{mU}$ - nominal value, **(D)** $S_S = 200 \frac{l}{mU}$.

FIGURE 7 | Plots of equilibrium T_4 and *TSH* levels depending on the thyroid's secretory capacity G_T. The red point in the figures indicates the nominal G_T-value from Ref. (1). **(A)** Equilibrium T_4, **(B)** equilibrium *TSH*.

G_T, i.e., from the thyroid's secretory capacity for T_4. Another interesting fact is that we can observe a small circadian rhythm in **Figure 8A** whereas the plot (**Figure 8B**) seems not to be affected by this. This confirms the observations we made in Section 3.1,

namely that incorporating intrathyroidal T_3-secretion causes a circadian rhythm in FT_3 and hence also in the sensitivity w.r.t. G_T.

As for T_4 and G_T, we can also analyze the stationary sensitivity $\lim_{t \to \infty} \frac{\partial FT_3}{\partial G_T}(t)$ for different values of G_T. In Ref. (10), the
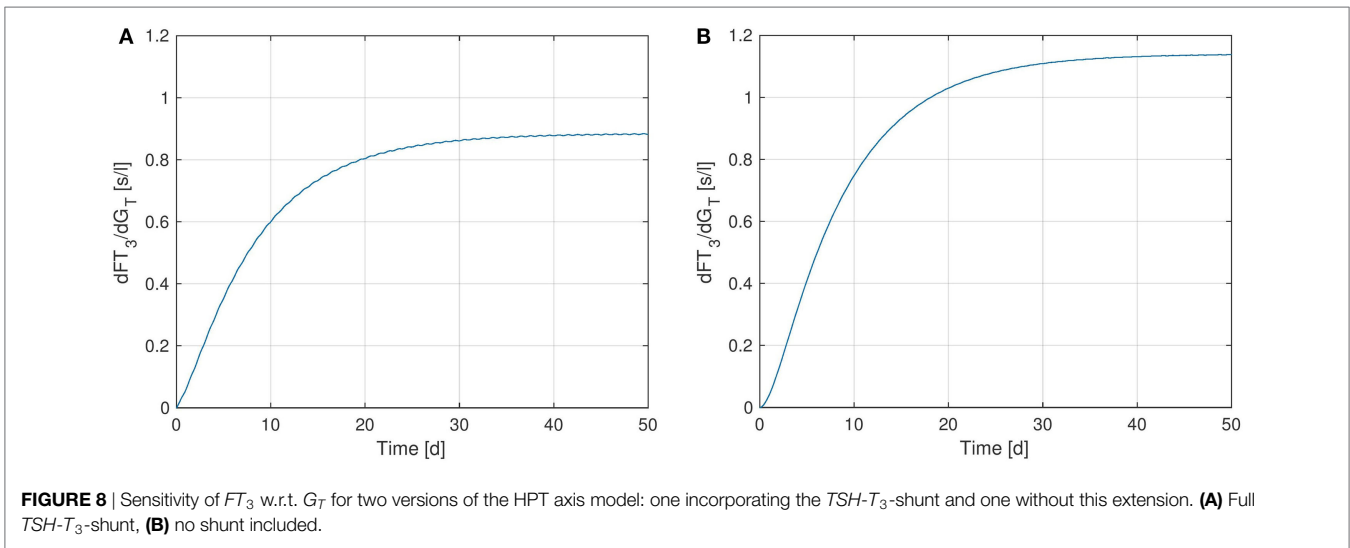
FIGURE 8 | Sensitivity of FT_3 w.r.t. G_T for two versions of the HPT axis model: one incorporating the TSH-T_3-shunt and one without this extension. **(A)** Full TSH-T_3-shunt, **(B)** no shunt included.
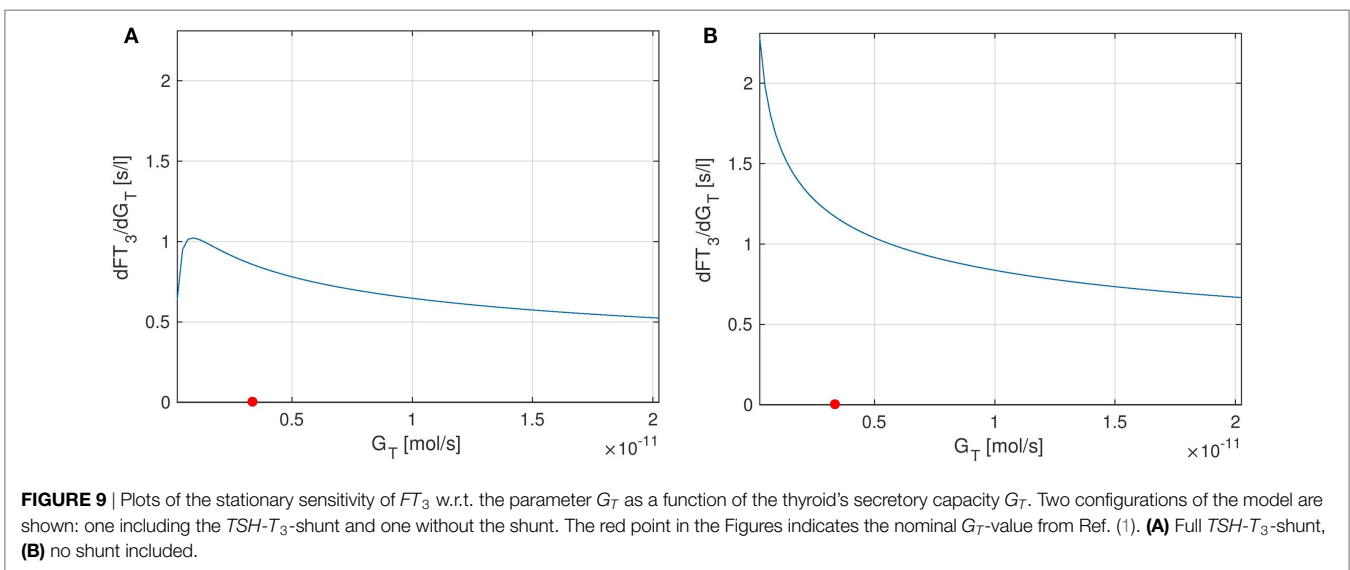

FIGURE 9 | Plots of the stationary sensitivity of FT_3 w.r.t. the parameter G_T as a function of the thyroid's secretory capacity G_T. Two configurations of the model are shown: one including the TSH-T_3-shunt and one without the shunt. The red point in the Figures indicates the nominal G_T-value from Ref. (1). **(A)** Full TSH-T_3-shunt, **(B)** no shunt included.

outcomes of a clinical study lead to the observation that the dependency of T_3-generation on G_T is lower than that predicted by a model, which does not include a TSH-T_3-shunt. Indeed, comparing **Figures 9A,B**, one can see that the sensitivity of FT_3 w.r.t. G_T significantly decreases when the shunt is incorporated into the model, i.e., T_3 production is less sensitive to fluctuations in the thyroid's secretory capacity if the shunt is included. As already mentioned above, this seems plausible since we now have a completely G_T-independent path from TSH to FT_3 (upper left block inside the thyroid in **Figure 1**).

5. CONCLUSION AND OUTLOOK

In this work, a mathematical model of the hypothalamic–pituitary–thyroid feedback loop was extended to include TSH-stimulated intrathyroidal T_3-secretion. The hypothesis of the existence of such a TSH-T_3-shunt has been brought forward in various recent clinical studies. Our results show

that the hypothesized mechanism can indeed explain various clinical findings. In particular, we have shown that intrathyroidal T_3-secretion results in a clear circadian pattern of peripheral FT_3, which has been observed *in vivo* in, e.g., Ref. (16, 19), and which is not the case without the incorporation of such a TSH-T_3-shunt. Also, a sensitivity analysis revealed that the sensitivity of peripheral FT_3 with respect to the thyroid's secretory capacity for T_4 is indeed lower when including intrathyroidal T_3-secretion into the model, in accordance with the clinical study of Ref. (10).

While the present report deals primarily with technical aspects of the thyroid pituitary feedback regulation, a better understanding of the underlying control system is of high clinical interest and relevance. Currently, clinical diagnosis and treatment of thyroid disease heavily relies on an indirect approach assessing the pituitary TSH response rather than circulating free thyroid hormones, FT_3 and FT_4 (21). The application is based on the underlying assumption that pituitary TSH in equilibrium at all times provides an accurate mirror image of the peripheral hormones. However,

recent evidence has challenged this simplistic tenet suggesting that the HPT axis is a much more dynamic system than has been previously thought (5, 22). In particular, the interrelationships between FT_3, FT_4, and TSH are less constantly fixed, rather conditional and contextualy adaptive (5, 22). Mathematical modeling presented in this study confirms and advances the theoretical framework that is emerging from recent clinical studies. Given the high prevalence of subclinical thyroid disorders in the population, being as high as 10% in middle aged women, the epidemiological and therapeutic implications are substantial. From the performed sensitivity analysis in the present study, important insights into the functionality of the HPT axis have been obtained. These include the robustification of TSH production through the ultrashort feedback loop in the pituitary, as well as a possible explanation why in clinical practice, diagnosis of wrong subclinical hypothyroidism is much more common than diagnosis of wrong subclinical hyperthyroidism.

In particular, the upper reference limit for TSH has been a matter of fierce debate for a decade (23). According to our models, the issue appears to be more fundamentally rooted. This relates to a substantial error rate, depending on the statistical analytical technique used, in the conventional disease classification based solely on statistical TSH abnormality (24). The relative variability in TSH rises even further with higher TSH concentrations in subclinical hypothyroidism (25). Recent guidelines have raised the clinical threshold for therapeutic intervention in subclinical hypothyroidism to a TSH level of 10 mU/l, whereas the laboratory-based disease definition continues to rely on the upper reference limit of approx. 4 mU/l (21). A better understanding and refined mathematical expression of hypothalamic–pituitary regulation in allostatic reactions (22), in thyrotropic insufficiency (26), and in situations of imminent thyroid failure (9, 27) as well as in their interactions may help reconcile this discrepancy that poses a considerable challenge to clinical decision-making.

Future work should focus on the further extension of the model to include currently unmodeled phenomena and mechanisms, such as, e.g., non-classical thyroid hormone signaling (28) and compartment models for the incorporation of membrane transport processes, which are increasingly understood as a regulatory element in their own right (29, 30). We would also aim to define the steady-state more narrowly and precisely for individual subjects under different conditions in an attempt to reduce the high uncertainty surrounding TSH measurements at the upper limit of its reference range. In general, obtaining further insight into the overall functionality of the hypothalamic–pituitary–thyroid feedback loop and developing suitable and detailed enough mathematical models might eventually pave the way for designing optimal medication strategies for various non-euthyroid states of human hormone homeostasis.

AUTHOR CONTRIBUTIONS

ACKNOWLEDGMENTS

FUNDING

SUPPLEMENTARY MATERIAL

The Supplementary Material for this article can be found online at https://www.frontiersin.org/articles/10.3389/fendo.2018.00091/full#supplementary-material.

REFERENCES

1. Dietrich JW. Der Hypophysen-Schilddrüsen-Regelkreis: Entwicklung und klinische Anwendung eines nichtlinearen Modells. In: Schardt F, editor. *Spektrum medizinischer Forschung* (Vol. 2), Berlin: Logos-Verlag (2002).
2. Dietrich JW, Tesche A, Pickardt CR, Mitzdorf U. Thyrotropic feedback control: evidence for an additional ultrashort feedback loop from fractal analysis. *Cybern Syst* (2004) 35(4):315–31. doi:10.1080/01969720490443354
3. Eisenberg M, Samuels M, DiStefano JJ III. Extensions, validation, and clinical applications of a feedback control system simulator of the hypothalamo-pituitary-thyroid axis. *Thyroid* (2008) 18(10):1071–85. doi:10.1089/thy.2007.0388
4. Dietrich JW, Landgrafe G, Fotiadou EH. TSH and thyrotropic agonists: key actors in thyroid homeostasis. *J Thyroid Res* (2012) 2012:29. doi:10.1155/2012/351864
5. Hoermann R, Midgley JE, Larisch R, Dietrich JW. Homeostatic control of the thyroid-pituitary axis: perspectives for diagnosis and treatment. *Front Endocrinol* (2015) 6:177. doi:10.3389/fendo.2015.00177
6. Hoermann R, Midgley JEM, Larisch R, Dietrich JW. Relational stability in the expression of normality, variation, and control of thyroid function. *Front Endocrinol* (2016) 7:142. doi:10.3389/fendo.2016.00142
7. Dietrich JW, Landgrafe-Mende G, Wiora E, Chatzitomaris A, Klein HH, Midgley JE, et al. Calculated parameters of thyroid homeostasis: emerging tools for differential diagnosis and clinical research. *Front Endocrinol* (2016) 7:57. doi:10.3389/fendo.2016.00057
8. Leow MK-S, Goede SL. The homeostatic set point of the hypothalamus-pituitary-thyroid axis – maximum curvature theory for personalized euthyroid targets. *Theor Biol Med Model* (2014) 11:35. doi:10.1186/1742-4682-11-35
9. Hoermann R, Midgley J, Dietrich J, Larisch R. Dual control of pituitary thyroid stimulating hormone secretion by thyroxine and triiodothyronine in athyreotic patients. *Ther Adv Endocrinol Metab* (2017) 8(6):83–95. doi:10.1177/2042018817716401
10. Hoermann R, Midgley JEM, Larisch R, Dietrich JW. Integration of peripheral and glandular regulation of triiodothyronine production by thyrotropin in untreated and thyroxine-treated subjects. *Horm Metab Res* (2015) 47(9):674–80. doi:10.1055/s-0034-1398616
11. Hoermann R, Midgley JEM, Larisch R, Dietrich JW. Is pituitary TSH an adequate measure of thyroid hormone-controlled homoeostasis during thyroxine treatment? *Eur J Endocrinol* (2013) 168:271–80. doi:10.1530/EJE-12-0819
12. Hoermann R, Midgley JEM, Giacobino A, Eckl WA, Wahl HG, Dietrich JW, et al. Homeostatic equilibria between free thyroid hormones and pituitary

thyrotropin are modulated by various influences including age, body mass index and treatment. *Clin Endocrinol* (2014) 81:907–15. doi:10.1111/cen.12527

13. Ishii H, Inada M, Tanaka K, Mashio Y, Naito K, Nishikawa M, et al. Induction of outer and inner ring monodeiodinases in human thyroid gland by thyrotropin. *J Clin Endocrinol Metab* (1983) 57:500–5. doi:10.1210/jcem-57-3-500

14. Beech SG, Walker SW, Arthur JR, Lee D, Beckett GJ. Differential control of type-I iodothyronine deiodinase expression by the activation of the cyclic AMP and phosphoinositol signalling pathways in cultured human thyrocytes. *J Mol Endocrinol* (1995) 14:171–7. doi:10.1677/jme.0.0140171

15. Morimura T, Tsunekawa K, Kasahara T, Seki K, Ogiwara T, Mori M, et al. Expression of type 2 iodothyronine deiodinase in human osteoblast is stimulated by thyrotropin. *Endocrinology* (2005) 146:2077–84. doi:10.1210/en.2004-1432

16. Russell W, Harrison RF, Smith N, Darzy K, Shalet S, Weetman AP, et al. Free triiodothyronine has a distinct circadian rhythm that is delayed but parallels thyrotropin levels. *J Clin Endocrinol Metab* (2008) 93(6):2300–6. doi:10.1210/jc.2007-2674

17. Pilo A, Iervasi G, Vitek F, Ferdeghini M, Cazzuola F, Bianchi R. Thyroidal and peripheral production of 3,5,3'-triiodothyronine in humans by multicompartmental analysis. *Am J Physiol* (1990) 258(4 Pt 1):E715–26.

18. Bianco AC, Salvatore D, Gereben B, Berry MJ, Larsen PR. Biochemistry, cellular and molecular biology, and physiological roles of the iodothyronine selenodeiodinases. *Endocr Rev* (2002) 23:38–89. doi:10.1210/edrv.23.1.0455

19. Jansen SW, Roelfsema F, van der Spoel E, Akintola AA, Postmus I, Ballieux BE, et al. Familial longevity is associated with higher TSH secretion and strong TSH-FT3 relationship. *J Clin Endocrinol Metab* (2015) 100(10):3806–13. doi:10.1210/jc.2015-2624

20. Khalil H. *Nonlinear Systems*. New York: Macmillan (1992).

21. Jonklaas J, Bianco AC, Bauer AJ, Burman KD, Cappola AR, Celi FS, et al. Guidelines for the treatment of hypothyroidism: prepared by the American thyroid association task force on thyroid hormone replacement. *Thyroid* (2014) 24(12):1670–751. doi:10.1089/thy.2014.0028

22. Chatzitomaris A, Hoermann R, Midgley JE, Hering S, Urban A, Dietrich B, et al. Thyroid allostasis-adaptive responses of thyrotropic feedback control to conditions of strain, stress and developmental programming. *Front Endocrinol* (2017) 8:163. doi:10.3389/fendo.2017.00163

23. Laurberg P, Andersen S, Carlé A, Karmisholt J, Knudsen N, Pedersen IB. The TSH upper reference limit: where are we at? *Nat Rev Endocrinol* (2011) 7(4):232–9. doi:10.1038/nrendo.2011.13

24. Hoermann R, Larisch R, Dietrich JW, Midgley JEM. Derivation of a multivariate reference range for pituitary thyrotropin and thyroid hormones: diagnostic efficiency compared with conventional single-reference method. *Eur J Endocrinol* (2016) 174:735–43. doi:10.1530/EJE-16-0031

25. Karmisholt J, Andersen S, Laurberg P. Variation in thyroid function tests in patients with stable untreated subclinical hypothyroidism. *Thyroid* (2008) 18(3):303–8. doi:10.1089/thy.2007.0241

26. Eisenberg MC, Santini F, Marsili A, Pinchera A, DiStefano JJ III. TSH regulation dynamics in central and extreme primary hypothyroidism. *Thyroid* (2010) 20(11):1215–28. doi:10.1089/thy.2009.0349

27. Falaschi P, Martocchia A, Proietti A, D'Urso R, Gargano S, Culasso F, et al. The hypothalamic-pituitary-thyroid axis in subjects with subclinical thyroid diseases: the impact of the negative feedback mechanism. *Neuro Endocrinol Lett* (2004) 25(4):292–6.

28. Flamant F, Cheng SY, Hollenberg AN, Moeller LC, Samarut J, Wondisford FE, et al. Thyroid hormone signaling pathways: time for a more precise nomenclature. *Endocrinology* (2017) 158(7):2052–7. doi:10.1210/en.2017-00250

29. Alkemade A, Friesema EC, Kalsbeek A, Swaab DF, Visser TJ, Fliers E. Expression of thyroid hormone transporters in the human hypothalamus. *J Clin Endocrinol Metab* (2011) 96(6):967–71. doi:10.1210/jc.2010-2750

30. Visser WE, Friesema EC, Visser TJ. Minireview: thyroid hormone transporters: the knowns and the unknowns. *Mol Endocrinol* (2011) 25(1):1–14. doi:10.1210/me.2010-0095